REGULAR ARTICLE

Theoretical study of the complex reaction of O(^{3}P) with trans-2-butene

Boulanouar Messaoudi · Sidi Mohamed Mekelleche ·
J. Raul Alvarez-Idaboy · Nelaine Mora-Diez

Abstract The complex potential energy surface for the reaction of triplet oxygen atom, O(^{3}P), with trans-2-butene is investigated at the MP2, PMP2, CCSD(T), CBS-4M and CBS-QB3 levels of theory. Both the O-addition and the two H-abstraction channels are thoroughly investigated. As expected, the calculations show that the O-addition is the most favourable process from a kinetic point of view. Various isomerization and dissociation pathways are explored following the addition of O(^{3}P) to trans-2-butene. Our calculations show that in the high-pressure limit, the major products are $CH_3CHC(O)H + CH_3$ (P1); whereas in the low-pressure limit the most thermodynamically stable products form: $CH_3CO + CH_3CH_2$ (P4). A more realistic prediction of reaction products is an intermediate case, being P1 more abundant followed by P4, in agreement with experimental data. The CBS-QB3 Gibbs free energies for the O-addition are smaller than those obtained at the CBS-4M level of theory, but the same general trends are obtained by these methods. The reaction and activation enthalpies, calculated at the CBS-QB3 level of theory, are in very good agreement with the experimental results available.

Keywords Atmospheric reactions · Triplet oxygen atoms · O(^{3}P) · Trans-2-butene · Potential energy surface · MP2 · CBS methods

B. Messaoudi · S. M. Mekelleche (✉)
Laboratoire de Thermodynamique Appliquée et Modélisation
Moléculaire, Département de Chimie, Faculté des Sciences,
Université A. Belkaid, BP 119, 13000 Tlemcen, Algeria
e-mail: sm_mekelleche@mail.univ-tlemcen.dz

B. Messaoudi · N. Mora-Diez (✉)
Department of Chemistry, Thompson Rivers University,
Kamloops, BC V2C 0C8, Canada
e-mail: nmora@tru.ca

J. R. Alvarez-Idaboy
Departamento de Física y Química Teórica, Facultad de
Química, Universidad Nacional Autónoma de México,
04510 Mexico, DF, Mexico

1 Introduction

There is considerable interest in performing both experimental and theoretical studies of the triplet oxygen atom reaction with saturated and unsaturated compounds due to the presence of several resulting radicals from these reactions in various combustion processes and atmospheric reactions [1–3]. Many experimental studies have tried to simulate the reaction conditions in different situations [4–10]. Formyl (HCO), acetyl (CH_3CO) and vinoxy (CH_2CHO) are some of the radicals of more concern. Due to their reactivity, these radicals have the ability to contribute to the production of tropospheric ozone [3].

The investigation of reaction channels, using theoretical approaches, contributes to a better understanding of reaction mechanisms and, therefore, to improve realistic conditions, such as combustion efficiency. The reaction of oxygen atoms in their ground electronic state O(^{3}P), with alkenes are important in understanding the combustion processes of hydrocarbons. The initial step of this reaction has been suggested to be the addition of the O(^{3}P) atom to the carbon–carbon double bond forming a biradical in the triplet state. Dating back to the early 1950s, Cvetanovic and co-workers carried out pioneering studies and have shown that the initial step of the reaction consists of an

attachment of the electrophilic O atom to the less substituted carbon atom of the double bond, forming an addition adduct, RCH$_2$CHCH$_2$O [11–17]. The prototype reaction, that is, O(^{3}P) with ethylene, has been extensively investigated over decades [18–30], mainly focusing on the competition between the various direct H-abstraction channels. Alkylation at one carbon atom makes the other one more likely to add an incoming O atom since a more stable biradical is to be formed. The allylic C–H bonds of the side chains are good targets for H-abstraction reactions. After a certain delay, the initially formed adduct falls apart, producing a variety of highly reactive radicals that are speedily converted into other species when in a hydrocarbon flame. Thus, in general, it is essentially impossible to determine the primary reaction products unless single-collision conditions are used [31]. The only single-collision experiments known to us on these reactions are the crossed molecular beam studies of Schmoltner et al. [7] on the O(^{3}P) reaction with ethylene and those of Anofsky et al. [10, 18]. on the reactions of O(^{3}P) with ethylene, propene and 1-butene. More recently, Bersohn's group [29–35] has performed a series of detailed studies of the reaction products of O(^{3}P) with alkenes. The triplet biradical, which forms following the addition of O(^{3}P) to the C = C bond, decomposes directly to a variety of final products [36]. Several channels corresponding to the O(^{3}P) attack on substituted alkenes H$_2$C = CHR (where R is an alkyl group) have been identified. For instance, it has been found that for the O(^{3}P) addition to ethylene, propene, and other alkenes (including 1-C$_4$H$_8$, cis-2-C$_4$H$_8$, iso-C$_4$H$_8$, 1-C$_5$H$_{10}$, allene, 1,3-C$_4$H$_6$, cyclopentene, and cyclohexene), the HCO channel branching ratios are 0.71 ± 0.16, 0.05 ± 0.02, and 0, respectively [32]. In order to explain these findings, it has been proposed that the H$_2$CO channel becomes more important as the hydrocarbon chain of the alkene increases since larger quantities of this substance are detected in these cases.

Oguchi et al. [36] have investigated the mechanism of the reaction of O(^{3}P) with three butene isomers (trans-2-, iso- and 1-butene) and have measured the yields of CH$_3$ and C$_2$H$_5$ radical products using photoionization mass spectrometry. For 1-butene, the fractions of CH$_3$ and C$_2$H$_5$ products are only 0.05 ± 0.01 and 0.29 ± 0.05, respectively. For trans-2-butene, these values are 0.52 ± 0.10 and 0.29 ± 0.05, respectively. The total fraction yield of the CH$_3$ and C$_2$H$_5$ products is 0.81. The rest of the channels accounting for the fraction of other products remain unclear. Zhao et al. [37] investigated the reaction pathways for the O(^{3}P) attack to iso-butene using the MP2 and CBS-4M methods, and they predicted the major product channels to be CH$_2$C(O)CH$_3$ + CH$_3$, cis/trans-CH$_3$CHCHO + CH$_3$, (CH$_3$)$_2$CCO + H$_2$ and CH$_3$C(CH$_2$)$_2$ + OH, with the (CH$_3$)$_2$CCO + H$_2$ channel being the most energetically

favourable. The channels leading to the formation of H + (CH$_3$)$_2$CCHO, HCO + (CH$_3$)$_2$CH, (CH$_3$)$_2$C + H$_2$CO, H + (CH$_3$)$_2$-CHCO, CO + (CH$_3$)$_2$CH$_2$ and (CH$_3$)$_2$CO + CH$_2$ are minor ones. Very recently, Zhao et al. [38]. have studied the reaction pathways of O(^{3}P) with 1-butene using the MP2 and G3 levels of theory. Their computational results indicate that the site selectivity of the addition of O(^{3}P) to either carbon atom of the double bond of 1-butene is not significant. The calculated heats of reaction at the G3 level for various product channels are in good agreement with the experimental data.

The theoretical method to be chosen to study the kinetics and the thermodynamics of the different reaction channels of these reactions should reproduce the experimental data available. The more substituted the alkene, the lower the activation energy for the O(^{3}P) addition. It is well known that several alkenes (e.g., trans- and cis-2-butene) have negative Arrhenius activation energies. Values between −1.20 and −2.66 kcal/mol have been reported for trans-2-butene [39–43].

Our aim in this paper is to perform a theoretical study of the different reaction channels of the reaction of O(^{3}P) with trans-2-butene exploring calculations at the MP2, PMP2, CCSD(T), CBS-4M and CBS-QB3 levels of theory. Both the addition and the two H-abstractions are thoroughly probed on the triplet potential energy surface, and the major products of these reactions are predicted. Several possible isomerisation and dissociation pathways following the addition reaction are explored. Calculated reaction and activation enthalpies are compared with available experimental data.

2 Computational details

Ab initio calculations were carried out with the Gaussian 03 suite of programs [44]. Using the Møller–Plesset perturbation theory truncated at the second order [45] in conjunction with the 6-311G(d,p) basis set, full geometry optimizations followed by frequency calculations at the same level of theory were performed for all the stationary points. Restricted (RMP2) and unrestricted (UMP2) methods were used for the closed and open-shell systems, respectively. Spin contamination of the open-shell systems was small. For the doublet radicals and the triplet biradicals, the expectation values of the total spin S^2 were <0.76 and 2.01, respectively, after spin annihilation. For the TSs, the spin contamination was slightly larger than for the other stationary points. Single-point energy calculations were performed at the CCSD(T)/6-311G(d,p) level of theory using the MP2 geometries. Additional calculations were performed using the CBS-4M [46, 47] and CBS-QB3 [47, 48] composite methods that employ HF/3-21G(d) and

B3LYP/6-311G(2d,d,p) geometries and frequencies, respectively, followed by a sequence of high-level single-point energy calculations and corrections designed to account for basis set truncations.

3 Results and discussions

The CBS-QB3 relative enthalpies and Gibbs free energies are reported in Table 1. The MP2/6-311G(d,p), PMP2/6-11G(d,p)//MP2/6-311G(d,p), CCSD(T)/6-311G(d,p)//MP2/6-311G (d,p), CBS-4M and CBS-QB3 relatives enthalpies and Gibbs free energies are reported in Table S1 of the Electronic Supplementary Material (ESM) section. The energies, various (MP2) thermal corrections, enthalpies and Gibbs free energies (in a.u. at 298.15 K) of the important stationary points along the trans-2-butene + O(^{3}P) addition and H-abstraction channels calculated at different levels of theory are reported in Table S2. The Cartesian coordinates of the CBS-QB3-optimized geometries of the stationary structures (reactant, intermediates, TSs and products) considered in the present study are reported in

the ESM section as well, along with the structures of the intermediates and TSs.

The best agreement with the experimental reaction enthalpies [36] is obtained with the CBS-QB3 method, with absolute deviations of 0.13–0.68 kcal/mol. The CBS-4M and PMP2 calculations have absolute deviations of 0.64–3.60 and 0.12–4.36 kcal/mol, respectively. The MP2- and CCSD(T)-calculated reaction enthalpies have larger errors. As it can be seen from Table 1, the reported experimental activation enthalpies for the addition step are negative, between −1.20 and −2.66 kcal/mol. Only the CBS methods are able to reproduce the expected negative sign. The CBS-QB3 result is in excellent agreement with experiment [43] (−2.32 kcal/mol), but the CBS-4M result is underestimated (−6.33 kcal/mol).

As clearly seen, the CBS-QB3 method is able to successfully reproduce the thermodynamic and kinetic data available for the reaction channels under study; hence, it can be used with confidence to calculate the mechanism of this reaction and to predict the thermodynamic and kinetic data not yet available. The CBS-4M method works reasonably well, but the MP2, PMP2 and CCSD(T) results

Table 1 Enthalpy and Gibbs free energy change (relative to the isolated reactants, in kcal/mol at 298.15 K) of important stationary points along the trans-2-butene + O(^{3}P) addition and H-abstraction channels calculated at the CBS-QB3 level of theory

	Relative enthalpy change		Relative gibbs free energy change
	$\Delta H_{CBS-QB3}$	ΔH_{exp}[b]	$\Delta G_{CBS-QB3}$
O(^{3}P) + trans-2-butene	0.00		0.00
CH$_3$CHCOH + CH$_3$ (P1)	−29.83	−29.19	−33.08
CH$_3$CHCOCH$_3$ + H (P2)	−23.89	−23.21	−24.81
CH$_3$CHO + CH$_3$CH (P3)	−11.81		−15.46
CH$_3$CO + CH$_2$CH$_3$ (P4)	−31.08	−30.86	−35.47
CH$_3$CH$_2$CO + CH$_3$ (P5)	−30.15	−29.90	−32.68
CH$_2$COCH$_3$ + CH$_3$ (P6)	−30.51	−30.38	−34.27
CH$_3$CHCHCH$_2$ + OH (P7)[a]	−15.94		−17.91
CH$_3$CHCCH$_3$ + OH (P8)[a]	5.52		2.99
^{3}IM1	−27.07		−19.68
^{3}IM2	−13.61		−10.98
^{3}IM3	−30.84		−30.84
^{3}IM4	−33.30		−25.37
		$\Delta H_{exp}^{\neq}$ [c]	
^{3}TS1	−2.32	[−1.20,−2.66]	5.34
^{3}TS2	−18.51		−11.17
^{3}TS3	−15.30		−7.35
^{3}TS4	−9.20		−3.20
^{3}TS5	−10.34		−5.28
^{3}TS6	−22.70		−15.38
^{3}TS7	−19.63		−12.39
^{3}TS8	−0.99		5.69
^{3}TS9 [a]	3.21		10.21
^{3}TS10 [a]	5.57		12.75

[a] Hydrogen abstraction products (P7 and P8) and TSs (TS9 and TS10)

[b] Experimental reaction enthalpies taken from Ref. [36]

[c] $\Delta H_{exp}^{\neq} = E_{aexp} - 2RT$, for bimolecular gas-phase reactions (Ref. [49]): −1.20 (Ref. [38] and [39]; $E_{a\ exp}$ = −0.02 kcal/mol); −1.54 (Ref. [40]; $E_{a\ exp}$ = −0.36 kcal/mol); −2.66 (Ref. [41]; $E_{a\ exp}$ = −1.48 kcal/mol)
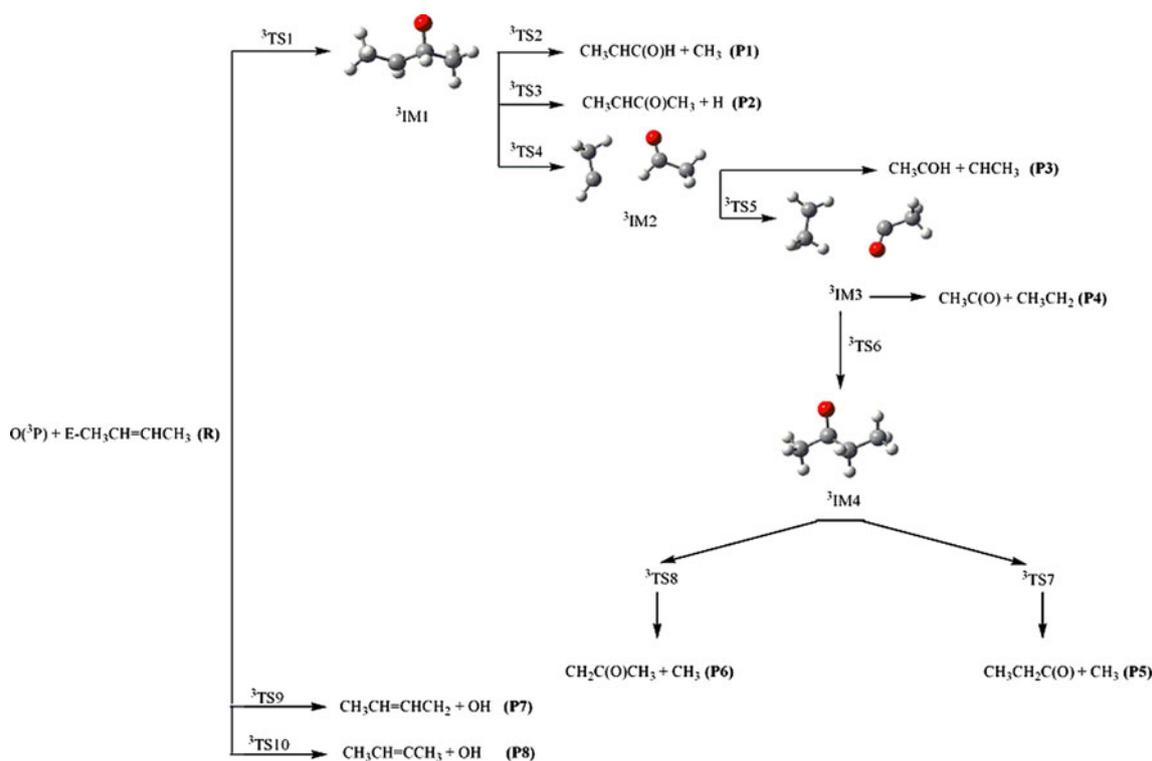
Scheme 1 Schematic representation of the different channels studied for the reaction of trans-2-butene with $O(^3P)$

should not be used to quantitatively study the thermodynamics and kinetics of the reactions of alkenes with $O(^3P)$. Spin contamination and its effect on the optimized MP2 geometries could be one of the reasons why the MP2, PMP2//MP2 and CCSD(T)//MP2 calculations are unable to reproduce the experimental data available. However, a few test calculations were performed using the CBS-QB3 geometries and frequency corrections combined with CCSD(T)/6-311G(d,p) single-point calculations and very similar relative enthalpies were obtained in comparison with the CCSD(T)//MP2 values reported in this paper (see Table S1). These results indicate that spin contamination on the MP2 geometries is not the main reason for the discrepancy with the experimental data.

The following subsections deal with the various pathways corresponding to the addition of $O(^3P)$ to trans-2-butene, the two possible H-abstractions and a comparison between these two channels. Scheme 1 provides a representation of the different channels considered.

3.1 The O-addition to trans-2-butene

Due to the symmetry of trans-2-butene, the addition of the $O(^3P)$ atom can occur at either of the two carbon atoms of the C=C bond. Figure 1 displays the potential energy profile of the adiabatic channels in the triplet state for the addition pathways calculated at the CBS-QB3 level of

theory, focusing on Gibbs free energy changes at 298.15 K. The structure of the different transition states (TSs) and intermediates are shown to facilitate the discussion that follows. The CBS-4M and CBS-QB3 results follow very similar qualitative trends; however, the CBS-QB3 Gibbs free energy barriers are smaller than the CBS-4M ones. The following discussions will focus on the CBS-QB3 Gibbs free energy data.

In Fig. 1, the first TS ($^3TS1$), which is 5.3 kcal/mol higher in G than the isolated reactants, corresponds to the addition of $O(^3P)$ to trans-2-butene, yielding the formation of the intermediate $^3IM1$, $CH_3C\cdot HCH(O\cdot)CH_3$. Three reaction channels follow the formation of this triplet adduct. The least energetic channel, with a barrier of 8.5 kcal/mol, leads to the formation of P1 ($CH_3CHC(O)H$ and CH_3, located at 33.1 kcal/mol below reactants) via $^3TS2$ (located 11.2 kcal/mol below reactants). $^3TS2$ results from the rupture of the C(O)–CH$_3$ bond in $^3IM1$. This channel corresponds to the lowest-energy decomposition pathway of $^3IM1$, which makes P1 the main products of the reaction investigated. Indeed, the formation of CH$_3$ in this reaction channel is in agreement with the experimental finding regarding the high CH$_3$ yield [36]. In addition, with a barrier of 12.3 kcal/mol, $^3IM1$ leads to the formation of the product P2 ($CH_3CHC(O)CH_3 + H$, located at 24.8 kcal/mol below reactants) via $^3TS3$ (which is at −7.4 kcal/mol relative to reactants). The third (more
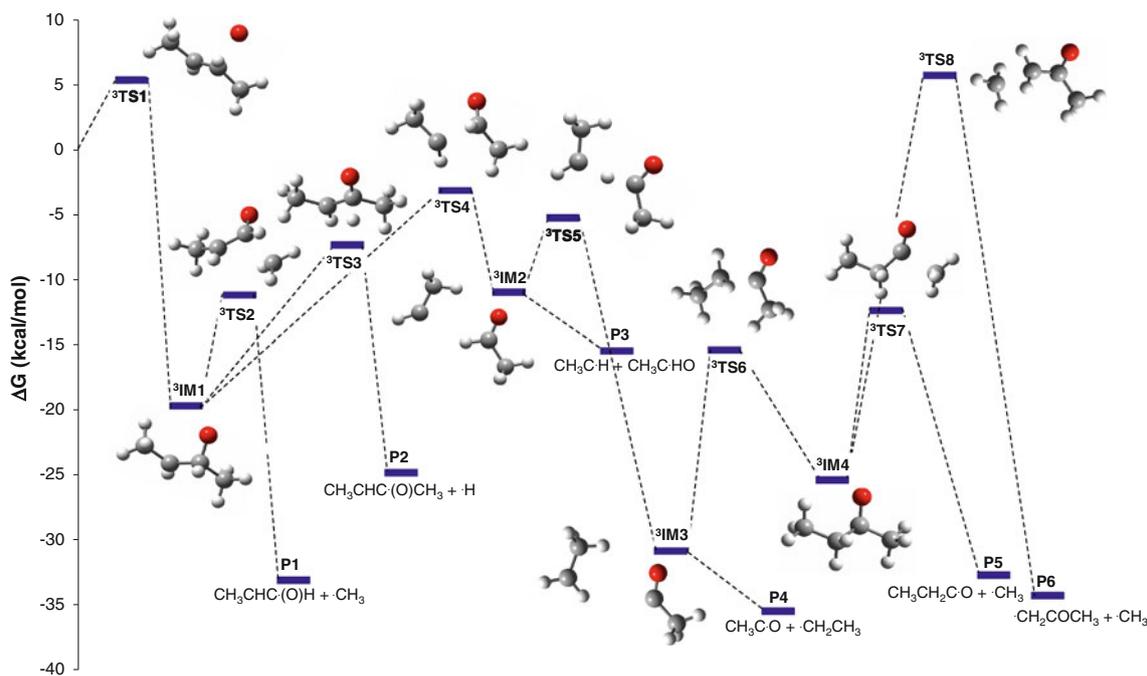
Fig. 1 Gibbs free energy profile of the adiabatic channels in the triplet state for the addition pathways of the reaction of trans-2-butene with O(^{3}P) calculated at the CBS-QB3 level of theory at 298.15 K

energetic) reaction channel from ^{3}IM1 involves the cleavage of the C–C bond between positions 2 and 3 to form the intermediate ^{3}IM2, via ^{3}TS4 (which is at −3.2 kcal/mol relative to reactants and 16.5 kcal/mol above ^{3}IM1). This intermediate, which is located at 11.0 kcal/mol below reactants, is the triplet complex formed between CH$_3$C˙H and CH$_3$C˙HO.

From ^{3}IM2, a third set of products (P3) could form (CH$_3$C˙H + CH$_3$C˙HO) which is 15.5 kcal/mol below reactants. Alternatively, depending on reaction conditions, a hydrogen abstraction could take place between the fragments of ^{3}IM2 via ^{3}TS5 (which is −5.3 kcal/mol relative to reactants) with a barrier of 14.4 kcal/mol. The product of this reaction is the triplet reactant complex between CH$_3$CH$_2$ and CH$_3$CO, and ^{3}IM3, which is 30.8 kcal/mol below reactants. Once ^{3}IM3 forms, the most realistic pathway to follow is the formation of P4 (CH$_3$CH$_2$ + CH$_3$CO), the most thermodynamically stable product of all the channels considered for the reaction under study (located at 35.5 kcal/mol below reactants). This calculation is in good agreement with the experimental findings of Oguchi et al. [36].

An alternative channel was considered that leads to the C–C bond formation between the fragments in ^{3}IM3 to form ^{3}IM4 (CH$_3$CH$_2$C˙(O˙)CH$_3$, located at 25.4 kcal/mol below reactants) via ^{3}TS6 (which is at −15.4 kcal/mol relative to reactants) with a barrier of 15.5 kcal/mol. There is a singlet TS for the 2,3-hydrogen shift connecting IM1 and IM4 on the singlet potential energy profile;

however, our calculations indicate that this TS does not exist in the triplet surface we are studying in this paper. From an energetic point of view, it is unlikely that ^{3}IM4 will form, but if it does, two fragmentation reaction channels could be considered that would increase the high overall yield of CH$_3$ in this reaction. ^{3}IM4 can dissociate to form P5 (CH$_3$CH$_2$CO + CH$_3$, located at 32.7 kcal/mol below reactants) via ^{3}TS7 by overcoming a barrier of 13.0 kcal/mol (^{3}TS7 is at −12.4 kcal/mol relative to reactants). Furthermore, ^{3}IM4 could form the product P6 (CH$_2$C(O)CH$_3$ + CH$_3$, which lies 34.3 kcal/mol below reactants) via ^{3}TS8 which is 31.1 kcal/mol above ^{3}IM4 (^{3}TS8 is at 5.7 kcal/mol relative to reactants).

It is worthy to note that the Gibbs free energy barrier from ^{3}IM1 to form H atoms (P2) is higher than that to form CH$_3$ radicals (P1), in agreement with the relative bond energy difference to break C–C and C–H bonds [31]. In general, Fig. 1 shows that the more stable a product, the lower the Gibbs free energy of its corresponding TS relative to the other reaction channels (P6 would be an exception). For example, P1 is more stable than P2, and this one is more stable than P3. The TSs leading to their formation follow the same energetic order. The barrier to form the most thermodynamically stable product (P4) is the smallest of all (the barrier between IM2 and TS5 is 5.7 kcal/mol) after the formation of ^{3}IM1. P4 is the most thermodynamically stable product because it leads to a more stable primary radical (e.g., CH$_2$CH$_3$ is more stable than CH$_3$).

The biradical adducts ^{3}IM1 (CH$_3$CHC(O)HCH$_3$) and ^{3}IM2 (CH$_3$CH$^{..}$CH$_3$CHO) are important intermediates in these reactions since they lead to the formation of the two most important reaction products, P1 and P4. Our calculations show that in the high-pressure limit, collisional stabilization leads to the formation of P1 (CH$_3$CHC(O)H + CH$_3$) as the major reaction product (the product that forms with the smallest reaction barrier). However, in the low-pressure limit, there is no collisional stabilization and everything with Gibbs free energies below ^{3}TS1 (the highest-energy point the system has overcome) can form (this would exclude the formation of ^{3}TS8 and P6). Hence, the reaction channel that leads to the most thermodynamically stable product, P4 in our case (CH$_3$CO + CH$_3$CH$_2$), predominates. A more realistic prediction of reaction products is an intermediate case in which there are some collisions that lead to some degree of stabilization, being P1 more abundant followed by P4, in agreement with the experimental data [36]. Close to the low-pressure limit, the formation of P2 (CH$_3$CHC(O)CH$_3$ + H) could compete due to tunnelling with the previously mentioned channels. At high pressures, P2 is not thermodynamically favoured.

3.2 The H-abstraction from trans-2-butene

Two possible O(^{3}P) H-abstraction pathways can be considered (see Scheme 1). When the O(^{3}P) atom attacks the H atom of the methyl group, the abstraction reaction proceeds via ^{3}TS9, with a barrier of 10.2 kcal/mol above reactants, leading to the formation of the product P7 (CH$_3$CH = CHCH$_2$ + OH, which lies at 17.9 kcal/mol below reactants). When the O(^{3}P) atom attacks the H atom attached to the C atom of the double bond, another abstraction reaction occurs via ^{3}TS10 surmounting a barrier of 12.8 kcal/mol and forming the product P8 (CH$_3$CH = CCH$_3$ + OH, which lies 3.0 kcal/mol above reactants). P7 is the most thermodynamically stable H-abstraction product. The H-abstraction from the CH$_3$ group is more favourable, as experimentally verified [31]. It can be clearly observed that the addition channel is much more favourable from a kinetic point of view than the H-abstraction channels (^{3}TS9 and ^{3}TS10 are 4.9 and 7.4 kcal/mol higher in Gibbs free energy than ^{3}TS1, respectively). Consequently, the H-abstraction channels should contribute only by a small fraction to the overall reaction.

4 Conclusions

In the present work, the different possible mechanisms of the complex multichannel reaction of O(^{3}P) with trans-2-butene are examined. The potential energy surface corresponding to the various reaction channels have been explored at the CBS-QB3, CBS-4M, CCSD(T), PMP2 and MP2 levels of theory. The calculated CBS-QB3 reaction and activation enthalpies are in very good agreement with the experimental data available, which gives us confidence in the calculated mechanism and in the quality of the predicted thermodynamic and kinetic data for this reaction at this level of theory.

O(^{3}P) atoms can attack either the carbon atom of the C=C bond or the hydrogen of the methyl group. The O-addition to the double bond is by far the most important reaction. This conclusion is in good agreement with the statements of Min et al. [33], indicating that the existence of extra side chains makes the addition of an O atom to a carbon atom of the double bond easier. As indicated some time ago by Cvetanovic [14–16], this is a consequence of the increased electronic density of the carbon atoms of the double bond. Our most realistic prediction of reaction products from the calculations presented in this paper lead to P1 (CH$_3$CHC(O)H + CH$_3$) as the most abundant product followed by P4 (CH$_3$CO + CH$_3$CH$_2$), in agreement with the experimental data [36].

References

1. Brider WC (1984) Combustion chemistry. Springer, New York
2. Cvetanovic RJ, Singelton DL (1984) Rev Chem Intermed 5:183
3. Finlayson-Pitts BJ, Pitts JN (1986) Atmospheric chemistry: fundamentals and experimental techniques. Wiley, New York
4. Loison JC, Dedonder-Lardeux C, Jouvet C, Solgadi D (1994) Faraday Discuss 97:379
5. Loison JC, Dedonder-Lardeux C, Jouvet C, Solgadi D (1992) Ber Bunsenges Phys Chem 96:1142
6. Loison JC, Dedonder-Lardeux C, Jouvet C, Solgadi D (1991) J Phys Chem 95:9192
7. Schmoltner AM, Chu PM, Brudzynski RJ, Lee YT (1989) J Chem Phys 91:6926
8. Moss MG, Hudgens JW, McDonald JD (1980) J Chem Phys 72:3486
9. Abou-Zied OK, McDonald JD (1998) J Chem Phys 109:1293
10. Kleinermanns J, Lutz AC (1981) J Phys Chem 85:1966
11. Cvetanovic RJ (1955) J Chem Phys 23:1375
12. Cvetanovic RJ (1955) Can J Chem 33:1684
13. Cvetanovic RJ (1956) J Chem Phys 25:376
14. Cvetanovic RJ (1959) J Chem Phys 30:19
15. Cvetanovic RJ (1960) J Chem Phys 33:1063
16. Cvetanovic RJ (1963) Adv Photochem 1:115
17. Cvetanovic RJ (1970) J Phys Chem 74:2730
18. Kanofsky JR, Gutman D (1972) Chem Phys Lett 15:236

19. Kanofsky JR, Lucas D, Gutman D (1973) Proc Symp Combust 14:285
20. Pruss FJ Jr, Slagle IR, Gutman D (1974) J Phys Chem 78:663
21. Hunziker HE, Kneppe H, Wendt HR (1981) J Photochem 17:377
22. Buss RJ, Baseman RJ, He G, Lee YT (1981) J Photochem 17:389
23. Sridharan UC, Kaufman F (1983) Chem Phys Lett 102:45
24. Smalley JF, Nesbitt FL, Klemm RB (1986) J Phys Chem 90:491
25. Endo Y, Tsuchiya S, Yamada C, Hirota E, Koda S (1986) J Chem Phys 85:4446
26. Koda S, Endo Y, Hirota E, Tsuchiya S (1987) J Phys Chem 91:5840
27. Bley U, Dransfeld P, Himme B, Koch M, Temps F, Wagner HG (1988) Proc Symp Combust 22:997
28. Knyazev VD, Arutyunov VS, Vedeneev VI (1992) Int J Chem Kinet 24:545
29. Anastasi C, Sanderson MG, Pagsberg P, Sillesen A (1994) J Chem Soc Faraday Trans 90:3625
30. Morton ML, Szpunar DE, Butler LJ (2001) J Chem Phys 115:204
31. Quandt R, Min Z, Wang X, Bersohn R (1998) J Phys Chem A 102:60
32. Min Z, Wong TH, Quandt R, Bersohn R (1999) J Phys Chem A 103:10451
33. Min Z, Wong TH, Su H, Bersohn R (2000) J Phys Chem A 104:9941
34. Su H, Bersohn R (2001) J Chem Phys 115:217
35. Su H, Bersohn R (2001) J Phys Chem A 105:9178
36. Oguchi T, Ishizaki A, Kakuta Y, Matsui H (2004) J Phys Chem A 108:1409
37. Zhao HM, Bian WS, Liu K (2006) J Phys Chem A 110:7858
38. Zhao HM, Pan L, Bian W (2012) Int J Quant Chem 112:858
39. Cvetanovic RJ (1987) J Phys Chem Ref Data 16:261
40. Singleton DL, Cvetanovic RJ (1976) J Amer Chem Soc 98:6812
41. Atkinson R, Pitts JN Jr (1977) J Chem Phys 67:38
42. Biehl H, Bittner J, Bohn B, Geers-Muller R, Stuhl F (1995) Int J Chem Kinet 27:277
43. Adusei GY, Fontijn A (1994) J Phys Chem 98:3732
44. Nakatsuji H, Hada M, Ehara M, Toyota K, Fukuda R, Hasegawa J, Ishida M, Nakajima T, Honda Y, Kitao O, Nakai H, Klene M, Li X, Knox JE, Hratchian HP, Cross JB, Bakken V, Adamo C, Jaramillo J, Gomperts R, Stratmann RE, Yazyev O, Austin AJ, Cammi R, Pomelli C, Ochterski JW, Ayala PY, Morokuma K, Voth GA, Salvador P, Dannenberg JJ, Zakrzewski VG, Dapprich S, Daniels AD, Strain MC, Farkas O, Malick DK, Rabuck AD, Raghavachari K, Foresman JB, Ortiz JV, Cui Q, Baboul AG, Clifford S, Cioslowski J, Stefanov BB, Liu G, Liashenko A, Piskorz P, Komaromi I, Martin RL, Fox DJ, Keith T, Al-Laham MA, Peng CY, Nanayakkara A, Challacombe M, Gill PMW, Johnson B, Chen W, Wong MW, Gonzalez C, Pople JA (2004) Gaussian 03; Revision E.01. Gaussian Inc, Pittsburgh
45. Møller C, Plesset MS (1934) Phys Rev 46:618
46. Ochterski JW, Petersson GA, Montgomery JA (1996) J Chem Phys 104:2598
47. Montgomery JA, Frisch MJ, Ochterski JW, Petersson GA (2000) J Chem Phys 112:6532
48. Montgomery JA, Frisch MJ, Ochterski JW, Petersson GA (1999) J Chem Phys 110:2822
49. Laidler KJ, Meiser JH, Sanctuary BC (2003) Physical chemistry, 4th Edition. Houghton